Lanthanide−Transition-Metal Carbonyl Complexes: New [Co$_4$(CO)$_{11}$]$^{2-}$ Clusters and Lanthanide(II) Isocarbonyl Polymeric Arrays

Christine E. Plečnik, Shengming Liu, Xuenian Chen, Edward A. Meyers, and Sheldon G. Shore*

Contribution from the Department of Chemistry, The Ohio State University, Columbus, Ohio 43210

Received August 7, 2003; E-mail: shore@chemistry.ohio-state.edu

Abstract: Two types of Ln(II)−Co$_4$ isocarbonyl polymeric arrays, {(Et$_2$O)$_{3-x}$(THF)$_x$Ln[Co$_4$(CO)$_{11}$]}$_\infty$ (**1**−**3**; x = 0, 1) and {(THF)$_5$Eu[Co$_4$(CO)$_{11}$]}$_\infty$ (**4**), were prepared and structurally characterized. Transmetalation involving Ln(0) and Hg[Co(CO)$_4$]$_2$ in Et$_2$O yields {(Et$_2$O)$_3$Ln[Co$_4$(CO)$_{11}$]}$_\infty$ (**1**, Ln = Yb; **2**, Ln = Eu). Dissolution of the solvent-separated ion pairs [Ln(THF)$_x$][Co(CO)$_4$]$_2$ (Ln = Yb, x = 6; Ln = Eu) in Et$_2$O affords {(Et$_2$O)$_2$-(THF)Yb[Co$_4$(CO)$_{11}$]}$_\infty$ (**3**) and {(THF)$_5$Eu[Co$_4$(CO)$_{11}$]}$_\infty$ (**4**). In these reactions, oxidation and condensation of the [Co(CO)$_4$]$^-$ anions result in formation of the new tetrahedral cluster [Co$_4$(CO)$_{11}$]$^{2-}$. The two types of Ln(II)−Co$_4$ compounds contain different isomers of [Co$_4$(CO)$_{11}$]$^{2-}$, and, consequently, the structures of the infinite isocarbonyl networks are distinct. The cluster in {(Et$_2$O)$_{3-x}$(THF)$_x$Ln[Co$_4$(CO)$_{11}$]}$_\infty$ (**1**−**3**) possesses pseudo C_{3v} symmetry (an apical Co, three basal Co atoms; one face-bridging, three edge-bridging, seven terminal carbonyls) and connects to Ln(II) centers through η^2,μ_4- and η^2,μ_3-carbonyls to generate a 2-D puckered sheet. In contrast, {(THF)$_5$Eu[Co$_4$(CO)$_{11}$]}$_\infty$ (**4**) incorporates a C_{2v} symmetric cluster (two unique Co environments; two face-bridging, one edge-bridging, eight terminal carbonyls), and isocarbonyl linkages (η^2,μ_4-carbonyls) to Eu(II) atoms create a 1-D zigzag chain. Complexes **1**−**4** contain the first reported η^2,μ_4-CO bridges between a Ln and a transition-metal carbonyl cluster. Infrared spectroscopic studies revealed that the isocarbonyl associations to Ln(II) persist in solution. The solution structure and dynamic behavior of the [Co$_4$(CO)$_{11}$]$^{2-}$ cluster in **1** was investigated by variable-temperature ^{59}Co and ^{13}C NMR spectroscopies.
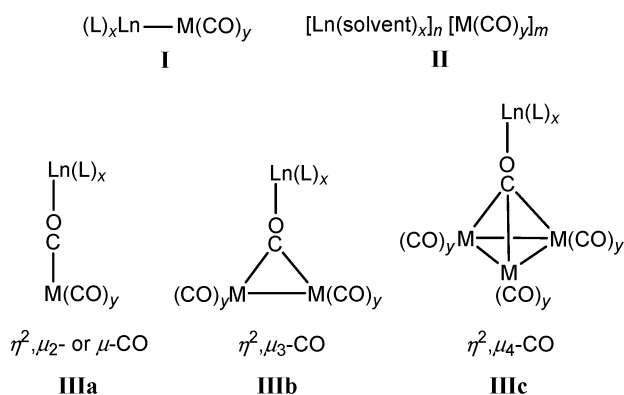
Introduction

Heterogeneous catalysts derived from lanthanide−transition-metal (Ln−M) cyanide compounds have demonstrated improved activity and selectivity over transition-metal only catalysts in important catalytic processes, such as the reduction of nitrogen oxides,[1a] vapor-phase hydrogenation of phenol,[1b] and hydrodechlorination of chlorobenzenes.[1c] The polymeric structural framework of these Ln−M cyanide catalyst precursors enables the uniform dispersion of the metals over the support's surface.[1a] For this reason, the design of catalyst precursors with Ln−M extended arraylike structures has been a priority in this laboratory. We are currently preparing potential[2] catalyst precursors derived from the heterometallic class of Ln−M carbonyls.[3] Over the last three decades, synthetic procedures toward Ln(II, III)−M carbonyl compounds were developed, and the structural relationship of the metal combinations was probed. Preparative methods[2b,4] for these heterometallics generally utilize simple

adduct formation,[5] metathesis,[5c,6,7] M−X bond cleavage,[8] M−M bond cleavage (1e$^-$ transfer,[4,6c,9] reduction in liquid ammonia,[10] amalgam reduction[11]), and transmetalation.[2c,6b,12,13] Cumulatively, these studies have revealed three possible kinds of Ln−M interactions (Chart 1): Ln−M direct bonds (**I**), solvent-separated ion pairs (**II**), and isocarbonyl linkages (**IIIa**−**IIIc**).

(1) (a) Rath, A.; Aceves, E.; Mitome, J.; Liu, J.; Ozkan, U. S.; Shore, S. G. *J. Mol. Catal. A* **2001**, *165*, 103. (b) Shore, S. G.; Ding, E.; Park, C.; Keane, M. A. *Catal. Commun.* **2002**, *3*, 77. (c) Jujjuri, S.; Ding, E.; Shore, S. G.; Keane, M. A. *Appl. Organomet. Chem.* **2003**, *17*, 493.
(2) (a) Beletskaya, I. P.; Voskoboinikov, A. Z.; Magomedov, G. K.-I. *Metalloorg. Khim.* **1989**, *2*, 814. (b) Beletskaya, I. P.; Voskoboinikov, A. Z.; Magomedov, G. K.-I. *Metalloorg. Khim.* **1990**, *3*, 516. (c) Lin, G.; Wong, W.-T. *J. Organomet. Chem.* **1996**, *522*, 271.
(3) Plečnik, C. E.; Liu, S.; Shore, S. G. *Acc. Chem. Res.* **2003**, *36*, 499.

(4) Evans, W. J.; Bloom, I.; Grate, J. W.; Hughes, L. A.; Hunter, W. E.; Atwood, J. L. *Inorg. Chem.* **1985**, *24*, 4620.
(5) (a) Marks, T. J.; Kristoff, J. S.; Alich, A.; Shriver, D. F. *J. Organomet. Chem.* **1971**, *33*, C35. (b) Crease, A. E.; Legzdins, P. *J. Chem. Soc., Chem. Commun.* **1972**, 268. (c) Crease, A. E.; Legzdins, P. *J. Chem. Soc., Dalton Trans.* **1973**, 1501. (d) Onaka, S.; Furuichi, N. *J. Organomet. Chem.* **1979**, *173*, 77. (e) Onaka, S. *Inorg. Chem.* **1980**, *19*, 2132.
(6) (a) Suleimanov, G. Z.; Beletskaya, I. P. *Dokl. Akad. Nauk SSSR* **1981**, *261*, 381. (b) Suleimanov, G. Z.; Khandozhko, V. N.; Shifrina, R. R.; Abdullaeva, L. T.; Kolobova, N. E.; Beletskaya, I. P. *Dokl. Akad. Nauk SSSR* **1984**, *277*, 1407. (c) Deng, D.; Zheng, X.; Qian, C.; Sun, J.; Dormond, A.; Baudry, D.; Visseaux, M. *J. Chem. Soc., Dalton Trans.* **1994**, 1665. (d) Hillier, A. C.; Sella, A.; Elsegood, M. R. J. *J. Chem. Soc., Dalton Trans.* **1998**, 3871.
(7) (a) Beletskaya, I. P.; Voskoboynikov, A. Z.; Chuklanova, E. B.; Kirillova, N. I.; Shestakova, A. K.; Parshina, I. N.; Gusev, A. I.; Magomedov, G. K.-I. *J. Am. Chem. Soc.* **1993**, *115*, 3156. (b) Magomedov, G. K.-I.; Voskoboynikov, A. Z.; Chuklanova, E. B.; Gusev, A. I.; Beletskaya, I. P. *Metalloorg. Khim.* **1990**, *3*, 706.
(8) (a) Crease, A. E.; Legzdins, P. *J. Chem. Soc., Chem. Commun.* **1973**, 775. (b) Beletskaya, I. P.; Suleimanov, G. Z.; Mekhdiev, R. Y.; Khandozhko, V. N.; Petrovskii, P. V.; Kolobova, N. E. *Dokl. Akad. Nauk SSSR* **1986**, *289*, 96. (c) Suleimanov, G. Z.; Khandozhko, V. N.; Mekhdiev, R. Y.; Petrovskii, P. V.; Kolobova, N. E.; Beletskaya, I. P. *Izv. Akad. Nauk SSSR, Ser. Khim.* **1986**, 1210. (d) Suleimanov, G. Z.; Khandozhko, V. N.; Mekhdiev, R. Y.; Petrovskii, P. V.; Yanovskaya, I. M.; Lependina, O. L.; Kolobova, N. E.; Beletskaya, I. P. *Izv. Akad. Nauk SSSR, Ser. Khim.* **1988**, 685.
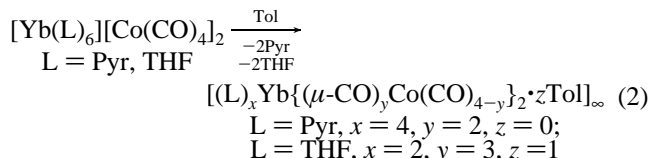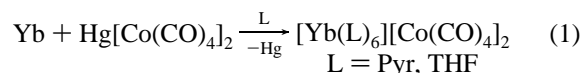
Chart 1

$$(L)_x Ln \!\!-\!\! M(CO)_y \qquad\qquad [Ln(solvent)_x]_n\,[M(CO)_y]_m$$
$$\textbf{I} \qquad\qquad\qquad\qquad \textbf{II}$$

$$\begin{array}{ccc}
Ln(L)_x & Ln(L)_x & Ln(L)_x \\
| & \diagup\;\diagdown & \\
O & O & O \\
\| & C & C \\
C & \diagup\;\diagdown & \\
| & & \\
M(CO)_y & (CO)_yM\!-\!M(CO)_y & (CO)_yM\!-\!M(CO)_y
\end{array}$$

$$\eta^2,\mu_2\text{- or }\mu\text{-CO} \qquad \eta^2,\mu_3\text{-CO} \qquad \eta^2,\mu_4\text{-CO}$$

$$\textbf{IIIa} \qquad\qquad \textbf{IIIb} \qquad\qquad \textbf{IIIc}$$

While it is difficult to separate kinetic and thermodynamic contributions to complex formation, the nature of the Ln−M bonding is highly contingent upon the nucleophilicity[14] of the transition metal in the carbonylate anion, $[M(CO)_y]^{n-}$. Specifically, the relative Lewis basicities of M, the CO ligands, and the solvent determine the type of interaction between Ln and M. Direct Ln−M bonded systems (**I**, Chart 1) are yielded when the transition-metal center is the most nucleophilic constituent (i.e., electron density resides on M).[7,10a,b] A solvent-separated ion pair (**II**) results when the electron-donating ability of the solvent exceeds that of $[M(CO)_y]^{n-}$.[4,6c,11c,13] If the carbonyl oxygens are more Lewis basic than M, then an isocarbonyl bridge (**IIIa−c**) to Ln is formed.[2c,6d,9] Low polarity or nonnucleophilic solvents can also favor the formation of an isocarbonyl even when $[M(CO)_y]^{n-}$ is a weak nucleophile.[9a,13] While the two types of isocarbonyl interactions η^2,μ_2-CO (μ-CO; **IIIa**)[2c,6d,9a,c,e,13] and η^2,μ_3-CO[9b,d] (**IIIb**) are known, Ln−M examples of η^2,μ_4-CO bridges (**IIIc**) have not been reported.[15]

Transmetalation (metal exchange reaction)[16] is a convenient synthetic route toward Ln−M carbonyls. We have demonstrated that transmetalation involving Yb and $Hg[Co(CO)_4]_2$ in strong coordinating solvents yields solvent-separated ion pairs, [Yb-$(L)_6][Co(CO)_4]_2$ (L = Pyr, THF; eq 1).[13] The strong nucleophilicity of the solvent, especially pyridine, hinders the pen-

(9) (a) Tilley, T. D.; Andersen, R. A. *J. Chem. Soc., Chem. Commun.* **1981**, 985. (b) Tilley, T. D.; Andersen, R. A. *J. Am. Chem. Soc.* **1982**, *104*, 1772. (c) Boncella, J. M.; Andersen, R. A. *Inorg. Chem.* **1984**, *23*, 432. (d) Boncella, J. M.; Andersen, R. A. *J. Chem. Soc., Chem. Commun.* **1984**, 809. (e) Hillier, A. C.; Liu, S. Y.; Sella, A.; Zekria, O.; Elsegood, M. R. J. *J. Organomet. Chem.* **1997**, *528*, 209.

(10) (a) Deng, H.; Shore, S. G. *J. Am. Chem. Soc.* **1991**, *113*, 8538. (b) Deng, H.; Chun, S.-H.; Florian, P.; Grandinetti, P. J.; Shore, S. G. *Inorg. Chem.* **1996**, *35*, 3891. (c) Voskoboinikov, A. Z.; Beletskaya, I. P. *Russ. Chem. Bull.* **1997**, *46*, 1789.

(11) (a) Suleimanov, G. Z.; Rybakova, L. F.; Abdullaeva, L. T.; Pasynskii, A. A.; Beletskaya, I. P. *Dokl. Akad. Nauk SSSR* **1983**, *272*, 885. (b) Beletskaya, I. P.; Suleimanov, G. Z.; Shifrina, R. R.; Mekhdiev, R. Y.; Agdamskii, T. A.; Khandozhko, V. N.; Kolobova, N. E. *J. Organomet. Chem.* **1986**, *299*, 239. (c) White, J. P., III; Deng, H.; Boyd, E. P.; Gallucci, J.; Shore, S. G. *Inorg. Chem.* **1994**, *33*, 1685.

(12) (a) Marianelli, R. S.; Durney, M. T. *J. Organomet. Chem.* **1971**, *32*, C41. (b) Suleimanov, G. Z.; Khandozhko, V. N.; Abdullaeva, L. T.; Shifrina, R. R.; Khalilov, K. S.; Kolobova, N. E.; Beletskaya, I. P. *J. Chem. Soc., Chem. Commun.* **1984**, 191. (c) Suleimanov, G. Z.; Khandozhko, V. N.; Petrovskii, P. V.; Mekhdiev, R. Y.; Kolobova, N. E.; Beletskaya, I. P. *J. Chem. Soc., Chem. Commun.* **1985**, 596.

(13) Plečnik, C. E.; Liu, S.; Liu, J.; Chen, X.; Meyers, E. A.; Shore, S. G. *Inorg. Chem.* **2002**, *41*, 4936.

(14) (a) King, R. B. *Acc. Chem. Res.* **1970**, *3*, 417. (b) Dessey, R. E.; Pohl, R. L.; King, R. B. *J. Am. Chem. Soc.* **1966**, *88*, 5121.

(15) For examples of η^2,μ_4-CO bridges between a Co cluster and a transition metal or a main group metal, please see: (a) Stutte, B.; Bätzel, V.; Boese, R.; Schmid, G. *Chem. Ber.* **1978**, *111*, 1603. (b) Merola, J. S.; Campo, K. S.; Gentile, R. A. *Inorg. Chem.* **1989**, *28*, 2950. (c) Schneider, J. J.; Denninger, U.; Krüger, C. *Z. Naturforsch.* **1994**, *49b*, 1549.

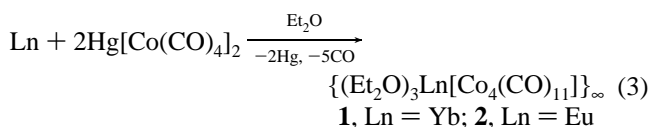(16) Burlitch, J. M.; Ferrari, A. *Inorg. Chem.* **1970**, *9*, 563.

etration of the weak nucleophile $[Co(CO)_4]^-$ into the Yb^{2+} coordination sphere.[17] It was also shown that the nonnucleophilic solvent toluene facilitates the transformation of the ion pairs into isocarbonyls, $[(L)_x Yb\{(\mu\text{-}CO)_y Co(CO)_{4-y}\}_2 \cdot z Tol]_\infty$ (eq 2).[13]

$$Yb + Hg[Co(CO)_4]_2 \xrightarrow[-Hg]{L} [Yb(L)_6][Co(CO)_4]_2 \quad (1)$$
$$L = \text{Pyr, THF}$$

$$[Yb(L)_6][Co(CO)_4]_2 \xrightarrow[\substack{-2Pyr \\ -2THF}]{Tol}$$
$$L = \text{Pyr, THF}$$

$$[(L)_x Yb\{(\mu\text{-}CO)_y Co(CO)_{4-y}\}_2 \cdot z Tol]_\infty \quad (2)$$
$$L = \text{Pyr, } x = 4, y = 2, z = 0;$$
$$L = \text{THF, } x = 2, y = 3, z = 1$$

These findings prompted the investigation of two reactions, transmetalation of Ln and $Hg[Co(CO)_4]_2$ and dissolution of the ion pairs $[Ln(THF)_x][Co(CO)_4]_2$, in Et_2O, which is a weak coordinating solvent and is less nucleophilic than $[Co(CO)_4]^-$.[17] Herein, we describe the remarkable influence that Et_2O imparts on these reactions, which involve oxidation and condensation of $[Co(CO)_4]^-$ anions into $[Co_4(CO)_{11}]^{2-}$ clusters. Two types of Ln(II)−Co$_4$ compounds, $\{(Et_2O)_{3-x}(THF)_x Ln[Co_4(CO)_{11}]\}_\infty$ (**1 − 3**; $x = 0, 1$) and $\{(THF)_5 Eu[Co_4(CO)_{11}]\}_\infty$ (**4**), are generated. The tetracobalt undecacarbonyl dianionic cluster, $[Co_4(CO)_{11}]^{2-}$, previously unknown,[18] exists in two isomeric forms and bonds to Ln(II) through isocarbonyl interactions to assemble 1-D or 2-D extended arrays. These complexes also contain the first reported η^2,μ_4-CO bridges between Ln and a transition-metal carbonyl cluster.

Results and Discussion

Transmetalation in Et$_2$O. Synthesis of $\{(Et_2O)_3 Ln[Co_4$-$(CO)_{11}]\}_\infty$ (1, Ln = Yb; 2, Ln = Eu). Transmetalation reactions (eq 3) involving 1:2 molar ratios of Ln metal (Ln = Yb, Eu) and $Hg[Co(CO)_4]_2$ in Et_2O afford $\{(Et_2O)_3 Ln[Co_4(CO)_{11}]\}_\infty$ (**1**, Ln = Yb; **2**, Ln = Eu; IUPAC formula, $[(Et_2O)_3 Ln\{(\eta^2,\mu_4$-$CO)(\eta^2,\mu_3$-$CO)_2 Co_4(\mu_2$-$CO)(CO)_7\}]_\infty$).

$$Ln + 2Hg[Co(CO)_4]_2 \xrightarrow[-2Hg, -5CO]{Et_2O}$$
$$\{(Et_2O)_3 Ln[Co_4(CO)_{11}]\}_\infty \quad (3)$$
$$\textbf{1}, Ln = Yb; \textbf{2}, Ln = Eu$$

During the reaction, oxidation of Ln(0) to Ln(II) and reduction of Hg(II) to Hg(0) take place. This is in accordance with other metal exchange reactions in strong coordinating solvents.[6b,11b,12b,13] Departure from these established Ln−Hg redox processes occurs with oxidation of the $[Co(CO)_4]^-$ anions (Co^{1-} to $Co^{1/2-}$) and condensation of the units to yield the tetracobalt undecacarbonyl dianionic cluster $[Co_4(CO)_{11}]^{2-}$. The formation of **1** and **2** distinctly contrasts transmetalation reactions that generate solvent-separated ion pairs $[Yb(L)_6][Co(CO)_4]_2$ (L = Pyr, THF; eq 1) in strong coordinating solvents.[13] Unlike the reactions that produce the ion pairs (complete in 12 h), transmetalation in Et_2O is slower, and **1** and **2** were obtained after several days (reactions were monitored by solution IR spectroscopy). Products **1** and **2** are 2-D heterometallic sheets supported by isocarbonyl bridges

(17) Darensbourg, M. Y. *Prog. Inorg. Chem.* **1985**, *33*, 221.

(18) Kemmitt, R. D. W.; Russell, D. R. In *Comprehensive Organometallic Chemistry*; Wilkinson, G., Stone, F. G. A., Abel, E. W., Eds.; Pergamon Press: New York, 1982; Vol. 8, p 8.
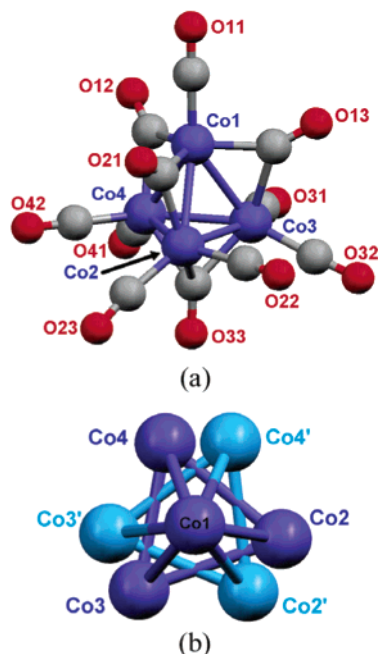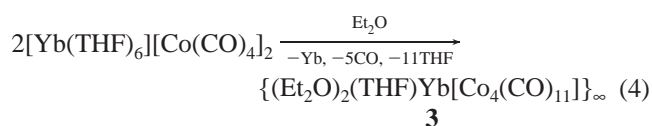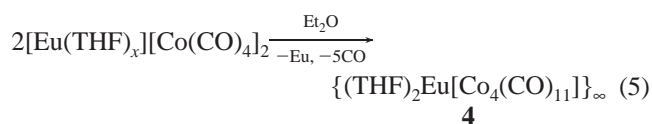
Figure 1. (a) Molecular structure of the $[Co_4(CO)_{11}]^{2-}$ cluster in $\{(Et_2O)_3\text{-}Yb[Co_4(CO)_{11}]\}_\infty$ (**1**). (b) View looking down on the disordered tetrahedral base.

between Ln(II) and the novel $[Co_4(CO)_{11}]^{2-}$ cluster, which has pseudo-C_{3v} symmetry (Figure 1a).

Dissolution of $[Ln(THF)_x][Co(CO)_4]_2$ in Et₂O. Formation of $\{(Et_2O)_2(THF)Yb[Co_4(CO)_{11}]\}_\infty$ (3) and $\{(THF)_5Eu[Co_4\text{-}(CO)_{11}]\}_\infty$ (4). To understand the cluster-building process in eq 3, the following reactions were carried out. The salt [Yb-(THF)₆][Co(CO)₄]₂ was stirred in Et₂O for several days, the volatiles were removed, and the mixture was stirred in fresh Et₂O for a day (eq 4). The latter two steps were repeated. Filtration of the red-brown colored solution and slow evaporation of the solvent produced crystals of $\{(Et_2O)_2(THF)Yb[Co_4\text{-}(CO)_{11}]\}_\infty$ (**3**; IUPAC formula, $[(Et_2O)_2(THF)Yb\{(\eta^2,\mu_4\text{-}CO)\text{-}(\eta^2,\mu_3\text{-}CO)_2Co_4(\mu_2\text{-}CO)(CO)_7\}]_\infty$).

$$2[Yb(THF)_6][Co(CO)_4]_2 \xrightarrow[-Yb, -5CO, -11THF]{Et_2O}$$
$$\{(Et_2O)_2(THF)Yb[Co_4(CO)_{11}]\}_\infty \quad (4)$$
$$\textbf{3}$$

In a slightly different procedure, [Eu(THF)$_x$][Co(CO)₄]₂ was stirred in Et₂O for several days, and much of it remained undissolved ([Eu(THF)$_x$][Co(CO)₄]₂, which is less soluble in Et₂O than [Yb(THF)₆][Co(CO)₄]₂). A minor quantity did react (eq 5), and the resulting red colored solution was filtered and crystals of $\{(THF)_5Eu[Co_4(CO)_{11}]\}_\infty$ (**4**; IUPAC formula, $[(THF)_5Eu\{(\eta^2,\mu_4\text{-}CO)_2Co_4(\mu_2\text{-}CO)(CO)_8\}]_\infty$) were isolated.

$$2[Eu(THF)_x][Co(CO)_4]_2 \xrightarrow[-Eu, -5CO]{Et_2O}$$
$$\{(THF)_2Eu[Co_4(CO)_{11}]\}_\infty \quad (5)$$
$$\textbf{4}$$

Although the starting materials in eqs 4 and 5 possess Ln(II) cations, redox/condensation reactions still transpire. One equivalent of Ln(II) is reduced to Ln(0), while [Co(CO)₄]⁻ anions are oxidized (Co^{1-} to Co$^{1/2-}$) and combined into $[Co_4(CO)_{11}]^{2-}$ clusters. This reactivity of the solvent-separated ion pairs in Et₂O

is in direct contrast to the dissolution of [Yb(THF)₆][Co(CO)₄]₂ in the nonnucleophilic solvent toluene, which does not cause redox/condensation (eq 2). Instead, displacement of some THF solvent ligands allows for the formation of isocarbonyl interactions between Yb(II) and [Co(CO)₄]⁻ to produce the 2-D sheetlike array $[(THF)_2Yb\{(\mu\text{-}CO)_3Co(CO)\}_2\cdot Tol]_\infty$.[13]

The structure of **3** is related to those of **1** and **2** even though the THF ligands were not completely replaced by Et₂O, and all three structures will be discussed collectively. Because of the low solubility of [Eu(THF)$_x$][Co(CO)₄]₂ in Et₂O, a slightly different procedure (volatiles were not completely removed, and fresh Et₂O was not added to the reaction mixture) was employed for the formation of **4**. This variation in procedure accounts for the dissimilar structures of **3** and **4** (no THF ligands were displaced by Et₂O). In fact, the $[Co_4(CO)_{11}]^{2-}$ cluster in **4** is an isomer of the cluster in **1**, **2**, and **3** because it has C_{2v} symmetry (Figure 6a). The extended structure of **4** is a 1-D zigzag chain that is sustained by isocarbonyl connections between $[Co_4(CO)_{11}]^{2-}$ and Eu(II).

Et₂O Facilitates the Formation of $[Co_4(CO)_{11}]^{2-}$. Diethyl ether is crucial for cluster generation (Scheme 1). The formation of **1** and **2** rather than solvent-separated ion pairs (eq 1) and the production of **3** and **4** instead of simple isocarbonyls (eq 2) can be attributed to the nucleophilicity and polarity of Et₂O. The solvent is weakly electron donating and is less nucleophilic than [Co(CO)₄]⁻ (decreasing order of donating ability: Pyr > THF ≈ [Co(CO)₄]⁻ > Et₂O > Tol).[17] In contrast to pyridine and THF (eq 1), Et₂O does not effectively separate the Ln(II) cation from the [Co(CO)₄]⁻ anion.[17] A covalent isocarbonyl interaction between [Co(CO)₄]⁻ and Ln(II) is plausible, but simple isocarbonyl complexes analogous to those prepared from the dissolution of the ion pairs in toluene ($[(THF)_2Yb\{(\mu\text{-}CO)_3Co(CO)\}_2\cdot Tol]_\infty$; eq 2) are not afforded. The polarity of Et₂O (more polar than toluene)[19] facilitates the oxidation and condensation of [Co(CO)₄]⁻. Essentially, cluster formation enhances the solubility of the products in Et₂O by reducing the net charge on the anion and delocalizing that charge over four metal centers. Also, as pointed out by a reviewer: "It is likely that potentials of the cobalt species are significantly different in these media and this could account better for the results."

To our knowledge, $[Co_4(CO)_{11}]^{2-}$ is a new cluster.[18] Reduction of Co₄(CO)₁₂ with alkali metals (Li, Na, K in THF),[20] cobaltocene (toluene),[20] and sodium carbide (THF)[21] produces $[Co_6(CO)_{14}]^{4-}$ and [Co(CO)₄]⁻. Also, Li[Co₃(CO)₁₀] is generated by the reaction of Li[Co(CO)₄] with Co₂(CO)₈ or Co₄(CO)₁₂ in Bu₂O and treatment of Co₂(CO)₈ with Li in Et₂O.[22] Other cluster complexes are formed when [Co(CO)₄]⁻ or Co₂(CO)₈ are combined with main group metal or early transition-metal reagents.[15,23]

Molecular Structures of 1−3. Single crystals of **1**, **2**, and **3** were grown from Et₂O solutions. Their colors, dark red-brown

(19) Jolly, W. L. *The Synthesis and Characterization of Inorganic Compounds*; Waveland Press: Prospect Heights, 1991; pp 100−101.
(20) (a) Chini, P.; Albano, V.; Martinengo, S. *J. Organomet. Chem.* **1969**, *16*, 471. (b) Albano, V. G.; Bellon, P. L.; Chini, P.; Scatturin, V. *J. Organomet. Chem.* **1969**, *16*, 461.
(21) Manning, M. C.; Trogler, W. C. *Inorg. Chim. Acta* **1981**, *50*, 247.
(22) (a) Faschinetti, G. *J. Chem. Soc., Chem. Commun.* **1979**, 397. (b) Fieldhouse, S. A.; Freeland, B. H.; Mann, C. D. M.; O'Brien, R. J. *J. Chem. Soc., Chem. Commun.* **1970**, 181.
(23) (a) Schwarzhans, K. E.; Steiger, H. *Angew. Chem., Int. Ed. Engl.* **1972**, *11*, 535. (b) Martin, J.; Fauconet, M.; Moïse, C. *J. Organomet. Chem.* **1989**, *371*, 87.
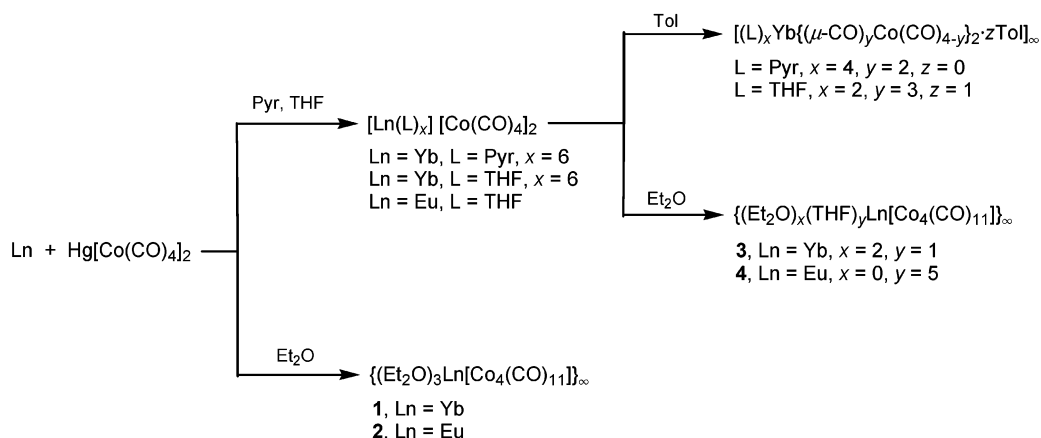
Scheme 1

```
                                                          Tol
                                                    ─────────►  [(L)ₓYb{(μ-CO)_yCo(CO)₄₋y}₂·zTol]_∞

                                                                L = Pyr, x = 4, y = 2, z = 0
                                                                L = THF, x = 2, y = 3, z = 1
                 Pyr, THF
          ────────────────►  [Ln(L)ₓ] [Co(CO)₄]₂ ──────
                             Ln = Yb, L = Pyr, x = 6
                             Ln = Yb, L = THF, x = 6
                             Ln = Eu, L = THF           Et₂O
                                                    ─────────►  {(Et₂O)ₓ(THF)_yLn[Co₄(CO)₁₁]}_∞

Ln + Hg[Co(CO)₄]₂ ──────                                       3, Ln = Yb, x = 2, y = 1
                                                               4, Ln = Eu, x = 0, y = 5

                 Et₂O
          ────────────────►  {(Et₂O)₃Ln[Co₄(CO)₁₁]}_∞

                             1, Ln = Yb
                             2, Ln = Eu
```

Table 1. Crystallographic Data for $\{(Et_2O)_3Yb[Co_4(CO)_{11}]\}_\infty$ (**1**), $\{(Et_2O)_3Eu[Co_4(CO)_{11}]\}_\infty$ (**2**), $\{(Et_2O)_2(THF)Yb[Co_4(CO)_{11}]\}_\infty$ (**3**), and $\{(THF)_5Eu[Co_4(CO)_{11}]\}_\infty$ (**4**)

	1	2	3	4
empirical formula	$C_{23}H_{30}O_{14}Co_4Yb$	$C_{23}H_{30}O_{14}Co_4Eu$	$C_{23}H_{28}O_{14}Co_4Yb$	$C_{31}H_{40}O_{16}Co_4Eu$
formula weight	939.26	918.15	937.21	1056.36
temp (K)	200	200	200	200
cryst size (mm)	$0.45 \times 0.27 \times 0.12$	$0.19 \times 0.15 \times 0.12$	$0.12 \times 0.08 \times 0.04$	$0.19 \times 0.12 \times 0.08$
cryst system	orthorhombic	orthorhombic	monoclinic	orthorhombic
space group	$Pbca$	$Pbca$	$P2_1/n$	$C222_1$
a (Å)	16.388(1)	16.381(1)	11.161(1)	12.472(1)
b (Å)	19.517(1)	19.720(1)	16.362(1)	17.246(1)
c (Å)	19.919(1)	20.095(1)	17.435(1)	18.045(1)
α (deg)	90	90	90	90
β (deg)	90	90	97.11(1)	90
γ (deg)	90	90	90	90
vol (Å³)	6371.1(6)	6491.3(6)	3159.3(4)	3881.4(4)
Z	8	8	4	8^a
ρ (calcd, g cm⁻³)	1.948	1.879	1.970	1.828
2θ limits (deg)	4.64−50.06	4.60−50.04	4.60−49.94	4.62−54.98
μ (mm⁻¹)	5.007	3.966	5.049	3.334
$R_1 [I > 2\sigma(I)]^b$	0.0417	0.0349	0.0518	0.0330
wR_2 (all data)^c	0.1205	0.0847	0.1376	0.1205
GOF on F^2	1.058	1.015	1.022	1.058

^{a} There is half of a molecule in the asymmetric unit. $^b R_1 = \sum||F_o| - |F_c||/\sum|F_o|$. $^c wR_2 = \{\sum w(F_o^2 - F_c^2)^2/\sum w(F_o^2)^2\}^{1/2}$.

or dark brown, are usual for polynuclear cobalt complexes. Compounds **1** and **2** are isomorphous. Compound **3** belongs to a different crystal system, but its structure is related to those of **1** and **2**. Molecular structures are illustrated in Figures 1−3. Crystallographic data and selected bond distances and angles are listed in Tables 1 and 2. The compounds consist of a $[Co_4(CO)_{11}]^{2-}$ cluster with pseudo-C_{3v} symmetry that bonds to Ln(II) atoms through isocarbonyl bridges to create 2-D sheets.

The tetrahedral tetracobalt dianionic cluster $[Co_4(CO)_{11}]^{2-}$ contains two distinct cobalt environments (Figure 1a). The apical cobalt, Co(1), is bonded to one terminal and three edge-bridging carbonyls, and the three basal cobalt atoms, Co(2), Co(3), and Co(4), are each connected to one face-bridging, one edge-bridging, and two terminal carbonyls. Mean Co−Co bond lengths (**1**, 2.481 Å; **2**, 2.479 Å; **3**, 2.479 Å) are consistent with $Co_4(CO)_{12}$ (avg., 2.490 Å).[24] The $Co_b−Co_b$[25] bonds (**1**, 2.462-(2)−2.476(2) Å) tend to be shorter than the $Co_a−Co_b$ bonds (**1**, 2.472(2)−2.524(2) Å). The edge-bridging carbonyls are

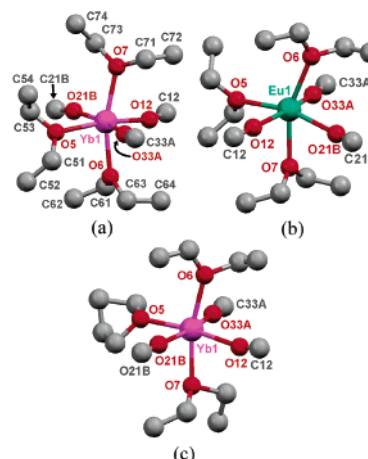(24) (a) Farrugia, L. J.; Braga, D.; Grepioni, F. *J. Organomet. Chem.* **1999**, *573*, 60. (b) Carré, F. H.; Cotton, F. A.; Frenz, B. A. *Inorg. Chem.* **1976**, *15*, 380. (c) Wei, C. H. *Inorg. Chem.* **1969**, *8*, 2384. (d) Wei, C. H.; Dahl, L. F. *J. Am. Chem. Soc.* **1966**, *88*, 1821.

(25) Subscripts represent the following types of Co atoms and CO ligands: a = apical, b = basal, t = terminal, e = edge-bridging, and f = face-bridging.

Figure 2. Coordination geometries about the Ln(II) centers in (a) $\{(Et_2O)_3Yb[Co_4(CO)_{11}]\}_\infty$ (**1**), (b) $\{(Et_2O)_3Eu[Co_4(CO)_{11}]\}_\infty$ (**2**), and (c) $\{(Et_2O)_2(THF)Yb[Co_4(CO)_{11}]\}_\infty$ (**3**). Hydrogen atoms on solvent ligands are omitted for clarity.

slightly asymmetric, with the $Co_a−C_e$ bonds (**1**, avg., 1.870 Å) being shorter than the $Co_b−C_e$ bonds (**1**, avg., 1.988 Å). The C−O distances increase according to the well-established order: $C−O_t$ (**1**, avg., 1.126 Å) < $C−O_e$ (avg., 1.176 Å) <
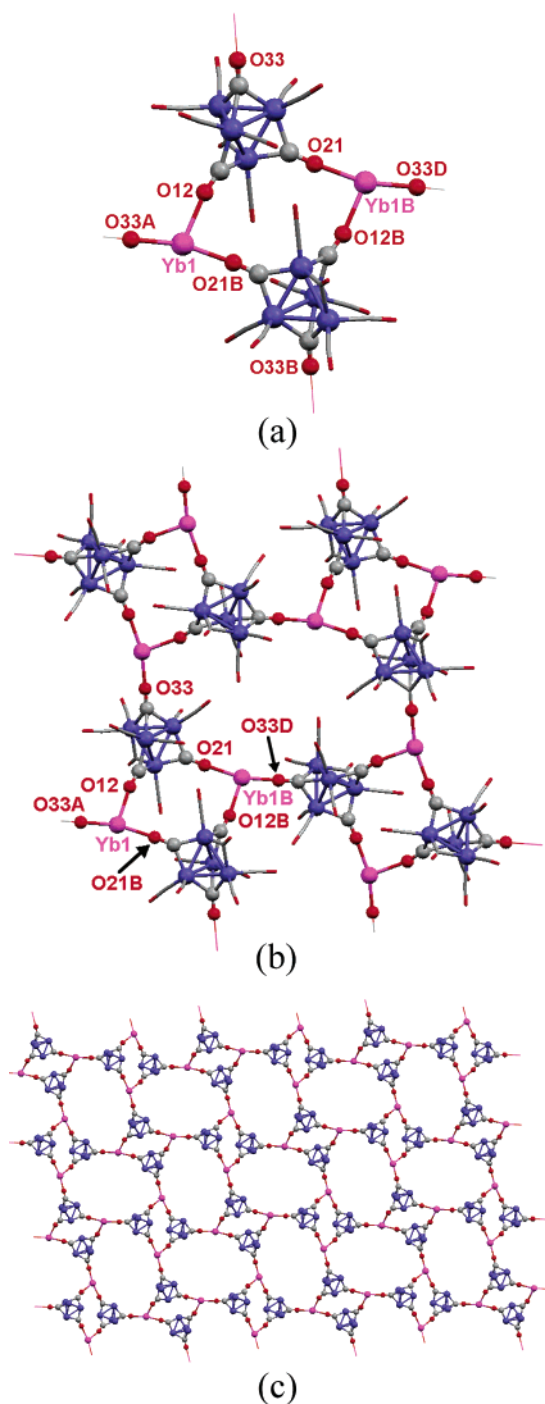
Figure 3. Molecular structures of the 2-D extended array of {(Et$_2$O)$_3$Yb-[Co$_4$(CO)$_{11}$]}$_\infty$ (**1**). (a) The "four-membered" ring building block, (b) the "eight-membered" ring building block, and (c) top view of the polymeric sheet. Et$_2$O ligands are omitted for clarity. Terminal and μ_2-carbonyls are represented as capped sticks in (a) and (b) and are omitted in (c).

Table 2. Selected Bond Distances and Bond Angles for {(Et$_2$O)$_3$Yb[Co$_4$(CO)$_{11}$]}$_\infty$ (**1**), {(Et$_2$O)$_3$Eu[Co$_4$(CO)$_{11}$]}$_\infty$ (**2**), and {(Et$_2$O)$_2$(THF)Yb[Co$_4$(CO)$_{11}$]}$_\infty$ (**3**)^{a,b}

	1	2	3
Ln(1)−O(5)	2.421(5)	2.538(3)	2.391(7)
Ln(1)−O(6)	2.409(5)	2.521(3)	2.402(9)
Ln(1)−O(7)	2.414(5)	2.539(4)	2.407(9)
Ln(1)−O(12)	2.411(5)	2.491(3)	2.390(8)
Ln(1)−O(21B)	2.385(5)	2.512(3)	2.377(6)
Ln(1)−O(33A)	2.318(5)	2.415(3)	2.315(6)
Co(1)−Co(2)	2.480(2)	2.463(1)	2.472(2)
Co(1)−Co(3)	2.524(2)	2.512(1)	2.516(2)
Co(1)−Co(4)	2.472(2)	2.494(1)	2.477(2)
Co(1)−C(11)	1.730(8)	1.738(5)	1.74(1)
Co(1)−C(12)	1.878(8)	1.855(5)	1.85(1)
Co(1)−C(13)	1.878(9)	1.864(6)	1.83(2)
Co(1)−C(21)	1.854(8)	1.875(5)	1.86(1)
Co(2)−C(21)	1.964(7)	1.951(5)	1.97(1)
Co(2)−C(33)	1.996(8)	2.020(5)	1.985(9)
Co(3)−C(13)	2.070(9)	2.069(5)	2.05(1)
Co(3)−C(33)	1.949(7)	1.950(5)	1.96(1)
Co(4)−C(12)	1.930(8)	1.950(5)	1.95(1)
Co(4)−C(33)	2.009(7)	1.974(5)	2.00(1)
C(11)−O(11)	1.150(9)	1.149(6)	1.15(1)
C(12)−O(12)	1.190(8)	1.188(6)	1.19(1)
C(13)−O(13)	1.147(10)	1.153(6)	1.27(3)
C(21)−O(21)	1.191(8)	1.182(6)	1.19(1)
C(33)−O(33)	1.217(8)	1.220(5)	1.22(1)
Ln(1)−O(12)−C(12)	163.1(5)	173.3(4)	157.8(8)
Ln(1)−O(21B)−C(21B)	170.6(5)	157.9(4)	177.8(7)
Ln(1)−O(33A)−C(33A)	175.2(5)	173.5(3)	178.3(7)
O(21B)−Ln(1)−O(12)	85.5(2)	88.0(1)	90.5(3)
O(12)−Ln(1)−O(33A)	109.0(2)	166.4(1)	101.9(3)
O(21B)−Ln(1)−O(33A)	165.3(2)	103.2(1)	167.2(2)

^{a} See Supporting Information for a molecular structure of the extended array. ^{b} Symmetry transformations used to generate equivalent atoms: **1**; (A) $x − \frac{1}{2}, −y + \frac{1}{2}, −z + 1$; (B) $−x + 1, −y + 1, −z + 1$; (D) $−x + \frac{3}{2}, −y + \frac{1}{2}, z$. **2**; (A) $−x + \frac{3}{2}, y + \frac{1}{2}, z$; (B) $−x + 1, −y, −z + 1$; (C) $x − \frac{1}{2}, −y − \frac{1}{2}, −z + 1$; (D) $−x + \frac{3}{2}, y − \frac{1}{2}, z$. **3**; (A) $−x + \frac{3}{2}, y − \frac{1}{2}, −z + \frac{3}{2}$; (B) $−x + 1, −y + 1, −z + 1$; (C) $x + \frac{1}{2}, −y + \frac{3}{2}, z + 1$; (D) $−x + \frac{3}{2}, y + \frac{1}{2}, −z + \frac{3}{2}$.

through Co$_a$ (Co(1)) and the tetrahedral base center. A complete description of this disorder is presented in the Supporting Information.

The Ln(II) atoms are six-coordinate, with three solvent ligands and three isocarbonyl oxygens arranged in a distorted octahedron (meridional isomer; Figure 2). Face- and edge-bridging carbonyl oxygens are more nucleophilic than terminal carbonyl oxygens.[17,26] Consequently, linkages exist between Ln(II) and the face- (CO(33)) and two edge-bridging (CO(12), CO(21)) carbonyls. The remaining edge-bridging carbonyl (CO(13)) does not engage in an isocarbonyl interaction. In all three complexes, the Ln−O$_f$(OC) distances (**1**, 2.318(5) Å) are shorter than both the Ln−O$_e$(OC) (**1**, 2.385(5), 2.411(5) Å) and Ln−O(Et$_2$O, THF) (**1**, 2.409(5)−2.421(5) Å) bond lengths. This reaffirms the stronger basicity of the methylidyne oxygen. The Ln−O−C bond angles associated with the face-bridging isocarbonyl connections were found to be almost linear, while those corresponding to the edge-bridging isocarbonyl bonds ranged from 157.8(8)−177.8(7)° (Table 2).

The outcome of the isocarbonyl linkages is a 2-D polymeric sheet (Figure 3c) that has two distinct building blocks. "Four-membered" rings, with two Ln(II) centers and two [Co$_4$(CO)$_{11}$]$^{2−}$

C−O$_f$ (1.217(8) Å).[26] A comparison of the terminal carbonyl lengths reveals that the Co$_a$−C$_t$ (**1**, 1.730(8) Å) and C−O$_{a,t}$ (**1**, 1.150(9) Å) bonds are shorter and longer, respectively, than the analogous basal distances (**1**, avg., Co$_b$−C$_t$, 1.767 Å; avg., C−O$_{b,t}$, 1.123 Å). In all three compounds, the basal cobalt atoms are disordered (Figure 1b).[24,27] These atoms adopt two sets of alternate positions that are related by rotation of an axis passing

(26) (a) Horwitz, C. P.; Shriver, D. F. *Adv. Organomet. Chem.* **1984**, *23*, 219. (b) De La Cruz, C.; Sheppard, N. *J. Mol. Struct.* **1990**, *224*, 141.

(27) (a) Albano, V. G.; Braga, D.; Longoni, G.; Campanella, S.; Ceriotti, A.; Chini, P. *J. Chem. Soc., Dalton Trans.* **1980**, 1820. (b) Duffy, D. N.; Mackay, K. M.; Nicholson, B. K.; Thomson, R. A. *J. Chem. Soc., Dalton Trans.* **1982**, 1029.

Table 3. IR Data in the Carbonyl Stretching Region

compound	medium	ν_{CO} (cm^{-1})
$\{(Et_2O)_3Yb[Co_4(CO)_{11}]\}_\infty$ (**1**)	Et$_2$O	2116 (vw), 2076 (vw), 2054 (w, sh), 2043 (mw), 2025 (m), 2008 (mw), 1994 (mw), 1936 (vs), 1849 (vw), 1744 (ms, br), 1613 (w, br)
	KBr	2075 (s, sh), 1982 (vs, br), 1852 (m, sh), 1793 (mw, sh), 1616 (mw)
$[^{13}C]\{(Et_2O)_3Yb[Co_4(CO)_{11}]\}_\infty$ ($[^{13}C]$**1**)	Et$_2$O	2101 (vw, sh), 2085 (vw), 2066 (vw, sh), 2047 (w, sh), 2018 (ms, sh), 2001 (s, sh), 1981 (vs), 1951 (m, sh), 1916 (mw, sh), 1894 (mw, sh), 1755 (w, br), 1726 (w, br), 1587 (w, br)
	KBr	1967 (vs, br), 1816 (s, sh), 1734 (ms, sh), 1653 (m, sh)
$\{(Et_2O)_3Eu[Co_4(CO)_{11}]\}_\infty$ (**2**)	Et$_2$O	2073 (m), 2057 (mw), 2042 (ms), 2019 (ms, sh), 2007 (vs), 1992 (s, sh), 1958 (mw, sh), 1928 (ms), 1852 (vw), 1783 (mw, br), 1612 (w, br)
	KBr	2068 (s, sh), 1977 (vs, br), 1869 (s, sh), 1786 (m, sh), 1676 (mw)
$\{(Et_2O)_2(THF)Yb[Co_4(CO)_{11}]\}_\infty$ (**3**)	Et$_2$O	2116 (w), 2076 (w, sh), 2053 (m, sh), 2028 (s), 1994 (vw, sh), 1931 (m, br), 1855 (w, sh), 1782 (mw, br), 1594 (w, br)
	KBr	2054 (ms, sh), 1994 (vs), 1971 (vs, br), 1950 (s, sh), 1930 (s, sh), 1855 (ms, sh), 1785 (m, sh), 1685 (m)
$\{(THF)_5Eu[Co_4(CO)_{11}]\}_\infty$ (**4**)	Et$_2$O^a	2116 (vw), 2065 (m, sh), 2054 (m), 2033 (ms), 2020 (m, sh), 2007 (m, sh), 1966 (w), 1924 (m, sh), 1900 (s, br), 1852 (ms, sh), 1786 (m)
	KBr	2054 (mw, sh), 1950 (vs), 1816 (mw), 1752 (w), 1707 (w)
$[Eu(THF)_x][Co(CO)_4]_2$	THF	2012 (mw), 1914 (vs), 1887 (ms, sh), 1809 (s)
	KBr	2055 (ms, sh), 2016 (s), 1933 (s), 1889 (s), 1851 (s), 1825 (s)

^{a} IR spectrum of a solution from which crystals of **4** were grown.

clusters, are constructed with edge-bridging isocarbonyl bonds (Figure 3a). The corner of the diamond-shaped ring is formed by the O(21B)−Ln(1)−O(12) angle that is almost 90°. Larger "eight-membered" rings (four Ln(II) centers, four $[Co_4(CO)_{11}]^{2-}$ clusters) have alternating face- and edge-bridging isocarbonyls bonds (Figures 3b). There are two O−Ln−O angles that build the oval-shaped, "eight-membered" rings. One angle (**1**, (O(12)−Yb(1)−O(33A)) is created by *cis*-isocarbonyl linkages, and these range from 85.5° to 109.0(2)°. The other angle (**1**, (O(21B)−Yb(1)−O(33A)) is formed by *trans*-isocarbonyl connections that are around 166° (Table 2).

Infrared Spectra of 1−3. Infrared spectra are presented in the Supporting Information. Isocarbonyl associations are clearly evident in IR spectra with ν_{CO} frequencies typically falling within the range of 1850−1300 cm^{-1}.[26] In general, ν_{CO} decreases according to the following types of isocarbonyl bridges: $\nu_{CO}(\eta^2,\mu_2$-CO) > $\nu_{CO}(\eta^2,\mu_3$-CO) > $\nu_{CO}(\eta^2,\nu_4$-CO).[26b] Infrared spectra (Table 3) of **1**, **2**, and **3** in Et$_2$O indicate that the isocarbonyl linkages are maintained in solution. There are several CO absorptions signifying that the $[Co_4(CO)_{11}]^{2-}$ anion has low symmetry. On the basis of the fact that isocarbonyl stretches appear at lower frequencies than bridging CO absorptions,[26b] we have tentatively assigned the CO stretching frequencies. Very low-frequency absorptions at 1613 cm^{-1} for **1** and 1612 cm^{-1} for **2** indicate the presence of η^2,μ_4-carbonyls (this stretch for **3** could not be positively identified). Edge-bridging isocarbonyl (η^2,μ_3-CO) bands are detected at 1744, 1783, and 1782 cm^{-1} for **1**, **2**, and **3**, respectively. For all of the compounds, weak absorptions at approximately 1850 cm^{-1} correlate to the edge-bridging carbonyls (μ_2-CO) not involved in isocarbonyl connections. Terminal CO stretches range from 2116 to 1928 cm^{-1}. Solid-state (KBr) IR spectra for the three complexes have a strong, broad terminal CO stretch centered at around 1980 cm^{-1} (a shoulder appears in the terminal stretching region between 2075 and 2054 cm^{-1}). The weaker bridging CO bands appear as shoulders to the terminal stretch (**1**; μ_2-CO, 1852 cm^{-1}; η^2,μ_3-CO, 1793 cm^{-1}; η^2,μ_4-CO, 1616 cm^{-1}).

For comparison, bridging CO stretches for some cobalt carbonyl clusters are listed: $Co_4(CO)_{12}$,[28] 1867 cm^{-1} (μ_2-CO); $[Co_6(CO)_{15}]^{2-}$, 1778 and 1737 cm^{-1} (μ_2-CO), 1685 cm^{-1} (μ_3-CO);[29] $[Co_6(CO)_{14}]^{,4-}$ 1680−1644 cm^{-1} (μ_3-CO).[20] Compounds with isocarbonyl linkages between a cobalt carbonyl and a Lewis acid have the following ν_{CO} frequencies: $[(Pyr)_4Yb\{(\mu$-CO)$_2$Co-(CO)$_2\}_2]_\infty$, 1776 cm^{-1} (Yb(II));[13] $[(THF)_2Yb\{(\mu$-CO)$_3$Co(CO)$\}_2\cdot$Tol]$_\infty$, 1784 cm^{-1} (Yb(II));[13] $Cp^*_2Yb(THF)\{(\mu$-CO)Co(CO)$_3\}$, 1761 cm^{-1} (Yb(III));[9a] $[(Cp^*_2Yb)_2\{(\eta^2,\mu_3$-CO)$_4Co_3$(C$_5H_4$-SiMe$_3$)$_2\}]$, 1575 cm^{-1} (Yb(III));[9d] $Cp_2Ti\{(\eta^2,\mu_4$-CO)$_4$Co$_3$-(CO)$_9\}_2$, 1375 and 1333 cm^{-1}.[15b]

^{59}Co and ^{13}C NMR Spectra of 1. The solution structure of the $[Co_4(CO)_{11}]^{2-}$ cluster in **1** was probed with ^{59}Co NMR spectroscopy.[30−32] The ambient temperature ^{59}Co NMR spectrum of **1** in d_{10}-Et$_2$O has a single resonance at −2910 ppm (Figure 4). Decreasing the temperature to −55 °C causes the signal to broaden, without the appearance of another peak. A slowing of the carbonyl exchange (vide infra) or a decrease in the ^{59}Co quadrupolar relaxation time would explain the broad-

(28) Bor, G. *Spectrochim. Acta* **1963**, *19*, 1209.
(29) (a) Chini, P.; Albano, V. *J. Organomet. Chem.* **1968**, *15*, 433. (b) Albano, V.; Chini, P.; Scatturin, V. *J. Organomet. Chem.* **1968**, *15*, 423.
(30) For references on ^{59}Co NMR spectroscopic studies of tetrahedral Co carbonyl clusters, please see: (a) Kempgens, P.; Raya, J.; Elbayed, K.; Granger, P.; Rosé, J.; Braunstein, P. *J. Magn. Reson.* **2000**, *142*, 64. (b) Granger, P.; Richert, T.; Elbayed, K.; Kempgens, P.; Hirschinger, J.; Raya, J.; Rosé, J.; Braunstein, P. *Mol. Phys.* **1997**, *92*, 895. (c) Kempgens, P.; Hirschinger, J.; Elbayed, K.; Raya, J.; Granger, P.; Rosé, J. *J. Phys. Chem.* **1996**, *100*, 2045. (d) Braunstein, P.; Mourey, L.; Rosé, J.; Granger, P.; Richert, T.; Balegroune, F.; Grandjean, D. *Organometallics* **1992**, *11*, 2628. (e) Song, L.-C.; Luo, C.-C.; Hu, Q.-M.; Chen, J.; Wang, H.-G. *Organometallics* **2001**, *20*, 4510.
(31) For references on ^{59}Co NMR spectroscopic studies of Co$_4$(CO)$_{12}$, please see: (a) Sizun, C.; Kempgens, P.; Raya, J.; Elbayed, K.; Granger, P.; Rosé, J. *J. Organomet. Chem.* **2000**, *604*, 27. (b) Aime, S.; Gobetto, R.; Osella, D.; Milone, L.; Hawkes, G. E.; Randall, E. W. *J. Magn. Reson.* **1985**, *65*, 308. (c) Haas, H.; Sheline, R. K. *J. Inorg. Nucl. Chem.* **1967**, *29*, 693. (d) Lucken, E. A. C.; Noack, K.; Williams, D. F. *J. Chem. Soc. A* **1967**, 148.
(32) For references on ^{59}Co NMR spectroscopy, please see: (a) Goodfellow, R. J. In *Multinuclear NMR*; Mason, J., Ed.; Plenum Press: New York, 1987; Chapter 20. (b) Laszlo, P. In *NMR of Newly Accessible Nuclei*; Laszlo, P., Ed.; Academic Press: New York, 1983; Vol. 2, Chapter 9. (c) Brevard, C.; Granger, P. *Handbook of High-Resolution Multinuclear NMR*; Wiley: New York, 1981; pp 124−125. (d) Kidd, R. G.; Goodfellow, R. J. In *NMR and the Periodic Table*; Harris, R. K., Mann, B. E., Eds.; Academic Press: New York, 1978; Chapter 8.
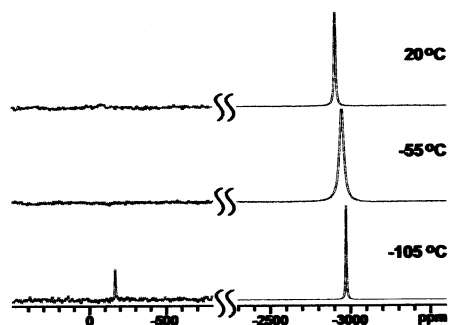
Figure 4. Variable-temperature ^{59}Co NMR spectra of $\{(Et_2O)_3Yb[Co_4-(CO)_{11}]\}_\infty$ (**1**) in d_{10}-Et$_2$O at 71.21 MHz.

ening.[33] In the −105 °C spectrum, a weak signal at −170 ppm is visible, and the upfield resonance has significantly sharpened.

On the basis of their temperature dependence and using the ^{59}Co chemical shifts of $Co_4(CO)_{12}$ as a guide (Co_a, −670 ppm; Co_b −2030 ppm),[31a] the two peaks may be designated. The apical cobalt resonance is unobservable at room temperature because of extensive line broadening induced by spin−spin coupling to the three basal cobalts.[33] However, lower temperatures cause "thermal decoupling" of the apical cobalt from the basal atoms, and both resonances sharpen noticeably.[34] Thermal decoupling results because the ^{59}Co quadrupolar relaxation time decreases at low temperatures.[35a] The ^{59}Co nuclei in $Co_4(CO)_{12}$ exhibit different temperature behavior.[31a]

A sample of **1** was enriched with ^{13}CO, such that the solution structure and dynamic behavior of the $[Co_4(CO)_{11}]^{2-}$ cluster could be examined by ^{13}C NMR spectroscopy. The variable-temperature ^{13}C NMR spectra of $[^{13}C]\{(Et_2O)_3Yb[Co_4(CO)_{11}]\}_\infty$ ($[^{13}C]$**1**; the excess ^{13}C may occur at any of the carbonyl positions) are illustrated in Figure 5. As the temperature is decreased, two phenomena are observed: (1) Thermal decoupling of the ^{13}C nuclei from the ^{59}Co nuclei takes place.[35] This causes terminal carbonyl resonances to narrow and two edge-bridging carbonyl (μ_2-CO, η^2,μ_3-CO) peaks to appear. (2) The intramolecular exchange process involving the basal terminal carbonyls slows, and the CO ligands begin to show inequivalence. Assignments of the carbonyl chemical shifts in **1** are based on the following two trends: $\delta(\mu_3$-CO$) > \delta(\mu_2$-CO$) > \delta($CO$_t)$[36] and bridging carbonyl signals are shifted downfield when a carbonyl oxygen binds with a Lewis acid (i.e., $\delta(\eta^2,\mu_3$-CO$) > \delta(\mu_2$-CO$)$).[37]

The room-temperature spectrum contains two broad terminal CO resonances at 214.7 and 204.2 ppm. The broad downfield signal is assigned to the six terminal basal carbonyls (C_b, C_c, C_d, $C_{d'}$), and the upfield peak belongs to the apical carbonyl (C_a). At −30 °C, the signal for C_a sharpens, the terminal basal peak resolves into two resonances (214.6 ppm, C_b, C_c; 208.3 ppm, C_d, $C_{d'}$), and another resonance emerges at 276.6 ppm for
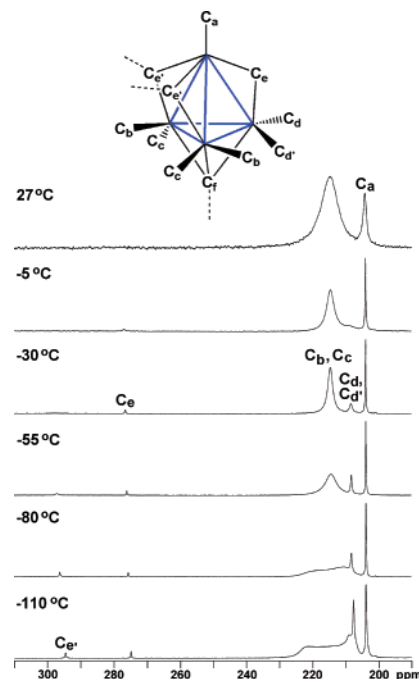
(33) Beall, H.; Bushweller, C. H. *Chem. Rev.* **1973**, *73*, 465.
(34) Beall, H.; Bushweller, C. H.; Dewkett, W. J.; Grace, M. *J. Am. Chem. Soc.* **1970**, *92*, 3484.
(35) (a) Evans, J.; Johnson, B. F. G.; Lewis, J.; Matheson, T. W.; Norton, J. R. *J. Chem. Soc., Dalton Trans.* **1978**, 626. (b) Aime, S.; Milone, L.; Osella, D.; Poli, A. *Inorg. Chim. Acta* **1978**, *30*, 45. (c) Aime, S.; Milone, L.; Valle, M. *Inorg. Chim. Acta* **1976**, *18*, 9. (d) Todd, L. J.; Wilkinson, J. R. *J. Organomet. Chem.* **1974**, *80*, C31.
(36) Chini, P.; Martinengo, S.; McCaffrey, D. J. A.; Heaton, B. T. *J. Chem. Soc., Chem. Commun.* **1974**, 310.
(37) (a) Wilkinson, J. R.; Todd, L. J. *J. Organomet. Chem.* **1976**, *118*, 199. (b) Hodali, H. A.; Shriver, D. F.; Ammlung, C. A. *J. Am. Chem. Soc.* **1978**, *100*, 5239. (c) Hodali, H. A.; Shriver, D. F. *Inorg. Chem.* **1979**, *18*, 1236.

Figure 5. Variable-temperature ^{13}C NMR spectra of $\{(Et_2O)_3Yb[Co_4-(CO)_{11}]\}_\infty$ (**1**) in d_{10}-Et$_2$O at 126 MHz and the low-temperature limiting structure of the cluster. The Co_4 core is represented by blue lines. Oxygen atoms are omitted. Dashed lines indicate isocarbonyl linkages. Atoms C_b and C_d are located approximately in the Co_3 basal plane, while C_c and $C_{d'}$ are positioned below the plane.

the μ_2-CO (C_e). In the −55 °C spectrum, the η^2,μ_3-CO ($C_{e'}$) peak is visible at 297.1 ppm. Line narrowing and the appearance of the edge-bridging CO resonances at low temperatures is attributed to thermal decoupling.[35] The η^2,μ_4-CO (C_f) signal is not observed at any temperature. If efficient thermal decoupling has not occurred, then the peak would remain broad due to coupling to the three quadrupolar ^{59}Co basal nuclei.

At −110 °C, the singlet for carbon atoms C_b and C_c separates into an unresolved multiplet with a broad complicated line shape (peaks at 220.1 and 209.2 ppm). The multiplet arises because the dynamic exchange of CO_b and CO_c has slowed. The average (214.7 ppm) of the multiplet peaks is consistent with the −30 °C chemical shift when the four carbonyls are equivalent. Interconversion of CO_d and $CO_{d'}$ is also expected. Slowing of this fluxional process is not clear from the spectra because the chemical shifts of the two inequivalent carbonyls would be similar.[38] It can be concluded that the static structure (Figure 5) of the $[Co_4(CO)_{11}]^{2-}$ cluster at the low-temperature limit is not reached.

As a reference, the ^{13}C resonances for $Co_4(CO)_{12}$ are located at 243.1 (μ_2-CO), 195.9 (CO$_t$), and 191.9 (CO$_t$) ppm.[35a] To the best of our knowledge, ^{13}C NMR resonances for face-bridging carbonyls in Co clusters have not been reported. Chemical shifts for face-bridging carbonyls in some Rh clusters are δ 241.6 for $[Cp_3Rh_3(\mu_3$-CO$)\{\eta^2,\mu_3$-C$_2$Ph$_2\}]$,[39] δ 237.4 for $[Rh_{12}(\mu_3$-CO$)_8-(\mu_2$-CO$)_2($CO$)_{20}]^{2-}$ (δ 211.5, μ_2-CO),[36] and δ 231−244 for $[Rh_6-(\mu_3$-CO$)_4($CO$)_{11}$X$]^-$ (X = I, CN, SCN).[40] The downfield shift

(38) A quantitative ^{13}C NMR experiment was performed at −110 °C (1024 scans, 0.130 s aquisition, 2 s pulse delay). The resonances were integrated, and the intensity ratio for the terminal carbonyls was 5.6:1 (basal:apical). The low intensities of the edge-bridging carbonyl resonances (1.1:1, $C_{e'}$:C_e) prevented their integration relative to the terminal carbonyls.
(39) Yamamoto, T.; Garber, A. R.; Bodner, G. M.; Todd, L. J.; Rausch, M. D.; Gardner, S. A. *J. Organomet. Chem.* **1973**, *56*, C23.
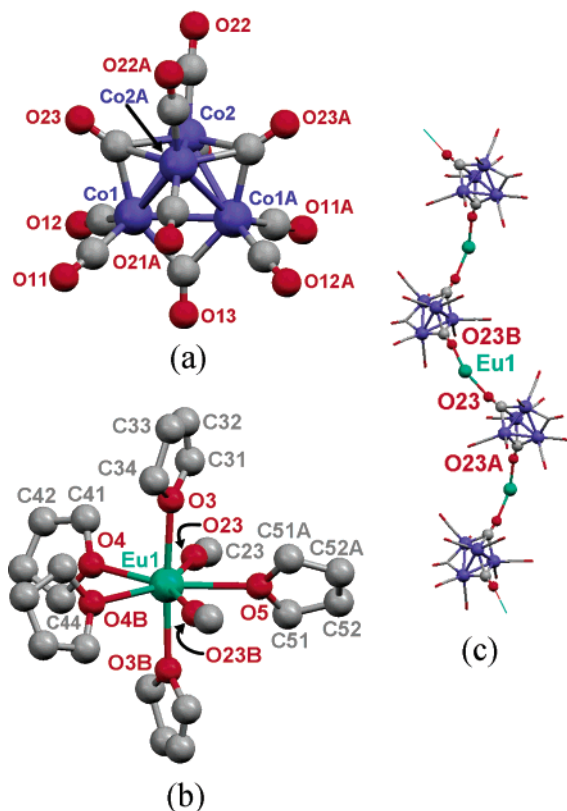
Figure 6. Molecular structures of $\{(THF)_5Eu[Co_4(CO)_{11}]\}_\infty$ (**4**). (a) The $[Co_4(CO)_{11}]^{2-}$ cluster. (b) Coordination geometry about the Eu(II) center (hydrogens attached to THF ligands are omitted for clarity). (c) A portion of the 1-D zigzag chain (THF ligands are omitted; terminal and edge-bridging carbonyls are represented as capped sticks).

Table 4. Selected Bond Distances (Å) and Angles (deg) for $\{(THF)_5Eu[Co_4(CO)_{11}]\}_\infty$ (**4**)[a]

Ln(1)−O(3)	2.519(3)	Ln(1)−O(4)	2.585(3)
Ln(1)−O(5)	2.590(4)	Ln(1)−O(23)	2.540(3)
Co(1)−Co(2)	2.4990(8)	Co(1)−Co(2A)	2.5118(8)
Co(1)−Co(1A)	2.574(1)	Co(2)−Co(2A)	2.365(1)
Co(1)−C(11)	1.767(5)	Co(1)−C(13)	1.945(6)
Co(1)−C(23)	1.925(5)	Co(2)−C(23)	2.031(4)
Co(2A)−C(23)	2.054(5)	C(11)−O(11)	1.138(6)
C(13)−O(13)	1.158(9)	C(23)−O(23)	1.189(5)
O(23)−Ln(1)−O(23B)	144.3(2)	Ln(1)−C(23)−O(23)	169.5(3)

[a] Symmetry transformations used to generate equivalent atoms: (A) x, $-y$, $-z + 1$; (B) $-x + 2$, y, $-z + \frac{1}{2}$.

of a carbonyl resonance upon complexation with a Lewis acid is exemplified by $[HFe_3(CO)_{11}]^-$.[37] The free anion has a bridging CO signal at 285.7 ppm (μ_2-CO), but in the presence of BF_3 the peak shifts to 355.1 ppm (η^2,μ_3-CO).[37a]

Molecular Structure of 4. Dark brown crystals of **4** were grown from a saturated Et_2O solution. The molecular structure is depicted in Figure 6. Crystallographic data and selected bond distances and angles are recorded in Tables 1 and 4. Complex **4** is composed of a C_{2v} symmetric $[Co_4(CO)_{11}]^{2-}$ cluster that coordinates to Eu(II) through isocarbonyl linkages to form a 1-D chain.

The asymmetric unit is comprised of the Eu(II) atom, 2.5 THF ligands, and half of the cluster. The entire tetrahedral cluster is generated by rotation of the two-fold crystallographic

(40) Allevi, C.; Bordoni, S.; Clavering, C. P.; Heaton, B. T.; Iggo, J. A.; Seregni, C.; Garlaschelli, L. *Organometallics* **1989**, *8*, 385.

axis that passes through CO(13) and the midpoints of the Co-(1)−Co(1A) and Co(2)−Co(2A) bonds (Figure 6a). There are two unique cobalt environments: Co(1) is bonded to one face-capping, one edge-bridging, and two terminal carbonyls, and Co(2) is attached to two face-bridging and two terminal CO ligands. The mean Co−Co bond length measures 2.494 Å. The Co−Co bonds (2.365(1)−2.5118(8) Å) that construct the faces capped by the oxymethylidyne carbonyls (CO(23), CO(23A)) are shorter than the Co(1)−Co(1A) distance (2.574(1) Å) that is spanned by one μ_2-CO (CO(13)). The Co−C_f (avg., 2.003 Å) and Co−C_e (1.945(6) Å) distances are elongated in comparison to the Co−C_t (avg., 1.756 Å) bonds. The face-bridging carbonyls are slightly asymmetric, because they are closer to Co(1) and Co(1A) (Co(1)−C(23), 1.925(5) Å; Co(2)−C(23), 2.031(4) Å; Co(2A)−C(23), 2.054(5) Å). Terminal C−O bonds (avg., 1.141 Å) are shortened relative to the edge- (1.158(9) Å) and face-bridging (1.189(5) Å) C−O bonds.

The Eu(II) center is seven-coordinate, with five THF ligands and two isocarbonyl oxygens arranged in a distorted pentagonal bypyramidal geometry (Figure 6b). Two THF ligands occupy the axial sites, while the isocarbonyl connections are located in the equatorial plane. The axial Eu(1)−O(THF) bonds (2.519-(3) Å) are shorter than the equatorial Eu(1)−O(THF) lengths (2.585(3), 2.590(4) Å). There is little distinction between the Eu(1)−O(THF) (2.519(3)−2.590(4) Å) and Eu(1)−O(23) (2.540-(3) Å) distances. This is in contrast to **1**, **2**, and **3**, in which the solvent ligands are less tightly bound to Ln(II) than the isocarbonyl oxygens. Isocarbonyl joints (η^2,μ_4-CO) occur only through the two face-bridging carbonyls (CO(23), CO(23A)). The outcome of the oxymethylidyne linkages is a 1-D zigzag chain (Figure 6c). The O(23)−Eu(1)−O(23B) angle associated with the isocarbonyl bonds is 144.3(2)°.

Infrared data for **4** are listed in Table 3. In the solid-state (KBr) IR spectrum, three weak low-frequency stretches are observed at 1816, 1752, and 1707 cm^{-1}. These are believed to be the μ_2- and η^2,μ_4-CO bands. A strong terminal CO stretch is detected at 1950 cm^{-1}. The IR spectrum of the solution from which crystals of **4** were grown is difficult to interpret (due to the low solubility of **4** in Et_2O, the solution was dilute). Two low-frequency CO stretches are observed at 1852 and 1786 cm^{-1}, and terminal CO absorptions range from 2116 to 1900 cm^{-1}.

Comparison of the Structural Features of 1−4. Tetracobalt undecacarbonyl dianion, $[Co_4(CO)_{11}]^{2-}$, is a typical 60 valence electron tetrahedron.[41] Although $[Co_4(CO)_{11}]^{2-}$ is isoelectronic with the neutral cluster $Co_4(CO)_{12}$, the increased negative charge encourages the formation of face-capping carbonyls.[42] The cluster in **1−3** (Isomer **A**) has one face- and three edge-bridging carbonyls, and the isomer in **4** (Isomer **B**) possesses one edge- and two face-bridging carbonyls (Chart 2). Dimensions of the Co_4 framework in Isomer **A** are comparable to those in Co_4-$(CO)_{12}$ (**1**, avgs., Co_a−Co_b, 2.492 Å, Co_b−Co_b, 2.470 Å; Co_4-$(CO)_{12}$, avgs., Co_a−Co_b, 2.499 Å, Co_b−Co_b, 2.482 Å).[24a] The symmetry of the Co_4 skeletal core in Isomer **B** is different from that of Isomer **A** and $Co_4(CO)_{12}$. While satisfying the Wade−Mingos rules, the cluster is a distorted tetrahedron.[41] The Co-

(41) Mingos, D. M. P.; May, A. S. In *The Chemistry of Metal Cluster Complexes*; Shriver, D. F., Kaesz, H. D., Adams, R. D., Eds.; VCH: New York, 1990; Chapter 2.

(42) Douglas, B.; McDaniel, D.; Alexander, J. *Concepts and Models of Inorganic Chemistry*, 3rd ed.; Wiley: New York, 1994; pp 857−859.

Chart 2

Co$_4$(CO)$_{12}$

[Rh$_4$(CO)$_{11}$]$^{2-}$

A

B
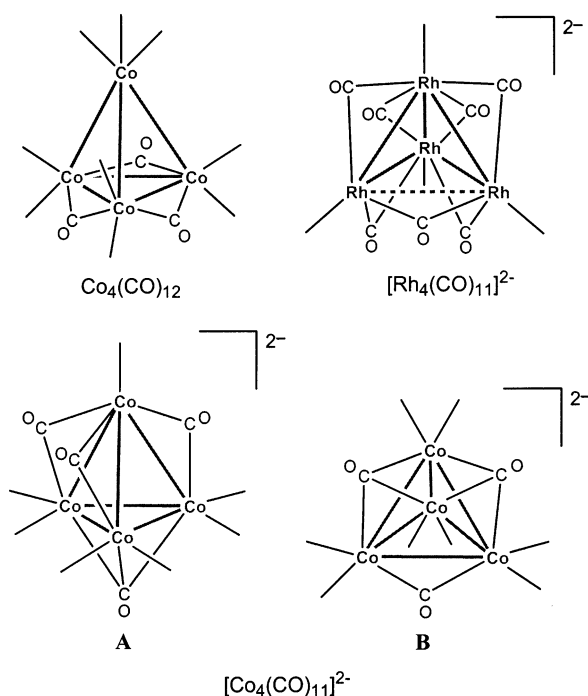
[Co$_4$(CO)$_{11}$]$^{2-}$

(2)−Co(2A), distance, 2.365(1) Å (Figure 6a) is unusually short, while the Co(1)−Co(1A) distance 2.574(1) Å, which is perpendicular to Co(2)−Co(2A), is longer than any other Co−Co length in **1**−**4** and Co$_4$(CO)$_{12}$. A point worthy of note is that the structure of [Rh$_4$(CO)$_{11}$]$^{2-}$ in the bis(triphenylphosphine)-iminum salt is also a distorted tetrahedron with an unusually long Rh−Rh distance but a different disposition of carbonyl ligands around the Rh$_4$ core.[50] Undoubtedly, as in the case of the [Co$_4$(CO)$_{11}$]$^{2-}$ cluster, the nature of the counterion plays a significant role in determining the arrangement of the carbonyl ligands and deviation from a regular tetrahedral core of [Rh$_4$(CO)$_{11}$]$^{2-}$. Note that [Rh$_4$(CO)$_{11}$]$^{2-}$ has no face-capping carbonyls, while the [Co$_4$(CO)$_{11}$]$^{2-}$ isomers do.

The inherent differences in symmetry of the **A** and **B** isomers cause the extended structures of **1**−**3** and **4** to be unique. In **1**−**3**, Isomer **A** coordinates to Ln(II) through the face-capping (η^2,μ_4) and two edge-bridging (η^2,μ_3) carbonyls, whereas in **4** isocarbonyl connections to Eu(II) occur only through the two face-bridging carbonyls of Isomer **B**. These are the first reported η^2,μ_4-CO bridges between a Ln and a transition-metal cluster. Isocarbonyl linkages in **1**−**3** generate a 2-D puckered sheet, and those in **4** produce a 1-D zigzag chain.

Conclusion

Two isomers of the new [Co$_4$(CO)$_{11}$]$^{2-}$ cluster were prepared. The clusters are present in two types of Ln(II)−Co$_4$ isocarbonyl extended arrays, $\{(Et_2O)_{3-x}(THF)_x Ln[Co_4(CO)_{11}]\}_\infty$ (**1**−**3**) and $\{(THF)_5 Eu[Co_4(CO)_{11}]\}_\infty$ (**4**). Compounds **1** and **2** were synthesized by the transmetalation reaction between Ln and Hg-[Co(CO)$_4$]$_2$ in Et$_2$O, and **3** and **4** were formed by dissolving [Ln(L)$_x$][Co(CO)$_4$]$_2$ in Et$_2$O. Diethyl ether, a weak donor solvent, permits the oxidation and condensation of the [Co(CO)$_4$]$^-$ anion to afford the [Co$_4$(CO)$_{11}$]$^{2-}$ cluster. This cluster is stable in Et$_2$O solution, as evidenced by ^{59}Co and ^{13}C NMR spectroscopies, and, furthermore, the isocarbonyl bonds between Ln(II) and [Co$_4$(CO)$_{11}$]$^{2-}$ persist in solution, based on ^{13}C NMR and IR

spectroscopic studies. The cluster in **1**−**3** has pseudo-C_{3v} symmetry and coordinates to Ln(II) centers, creating a 2-D sheet. On the other hand, the [Co$_4$(CO)$_{11}$]$^{2-}$ isomer in **4** has C_{2v} symmetry and bonds to Eu(II) to generate a 1-D zigzag chain. The η^2,μ_4 isocarbonyl bridges in **1**−**4** are the first reported for a Ln and transition-metal carbonyl cluster.

Experimental Section

General Data. All manipulations were carried out on a standard high vacuum line or in a drybox under an atmosphere of nitrogen unless otherwise noted. Diethyl ether and tetrahydrofuran were dried and stored over sodium/benzophenone and freshly distilled prior to use. Hexane was stirred over concentrated sulfuric acid for 2 d and then decanted and washed with water. Next, the hexane was stirred over sodium/benzophenone for 7 d, followed by distillation into a storage bulb containing sodium/benzophenone. Celite was dried by being heated at 150 °C under dynamic vacuum for 5 h. Ytterbium powder (Strem) was used as received. Europium ingot (Aldrich) was received in mineral oil, washed in hexane, and vacuum-dried. ^{13}CO (99% enriched) was purchased from Isotec. Sodium tetracarbonylcobaltate,[43] bis(cobalt tetracarbonyl)mercury,[13,44] and [Yb(THF)$_6$][Co(CO)$_4$]$_2$[13] were prepared according to the previously published methods. Elemental analyses were performed by Galbraith Laboratories (Knoxville, TN). Prolonged pumping on crystalline samples caused loss of not only solvent ligands but also carbon monoxide. Therefore, analyses are calculated for the loss of solvent and CO. They reflect instabilities in a vacuum at room temperature. Infrared spectra were recorded on a Mattson Polaris Fourier transform spectrometer with 2 cm^{-1} resolution. Refer to Table 3 for IR data. Infrared spectra are reported in the Supporting Information. ^{1}H NMR spectra were obtained on Bruker AM-250 and DPX-400 spectrometers operating at 250.1 and 400.1 MHz and were referenced to residual solvent protons. ^{13}C NMR spectra were obtained on a Bruker DRX-500 NMR spectrometer operating at 125.8 MHz and were referenced to deuterated solvent signals. ^{59}Co NMR spectra were obtained on a Bruker DMX-300 NMR spectrometer operating at 71.21 MHz and were externally referenced to K$_3$[Co(CN)$_6$] in D$_2$O ($\delta = 0.00$ ppm). Standard parameters are as follows: pulse width 8.2 μs, sweep width 100 kHz, and number of scans between 500 and 10 000.

X-ray Structure Determinations. Single-crystal X-ray diffraction data were collected on a Nonius KappaCCD diffraction system which employs graphite-monochromated Mo Kα radiation ($\lambda = 0.71073$ Å). A single crystal of **1**, **2**, **3**, and **4** was mounted on the tip of a glass fiber coated with Fomblin oil (a pentafluoropolyether). Unit cell parameters were obtained by indexing the peaks in the first 10 frames and were refined employing the whole data set. All frames were integrated and corrected for Lorentz and polarization effects using the DENZO-SMN package (Nonius BV, 1999).[45] Absorption correction was applied using the SORTAV program[46] provided by MaXus software.[47] The positions of the heavy atoms, Yb, Eu, and Co, were revealed by the Patterson method. The structures were refined using the SHELXTL-97 (difference electron density calculation, full-matrix least-squares refinements) structure solution package.[48] Data merging was perfomed using the data preparation program supplied by

(43) Edgell, W. F.; Lyford, J., IV. *Inorg. Chem.* **1970**, *9*, 1932.

(44) Ruff, J. K.; Schlientz, W. J. *Inorg. Synth.* **1974**, *15*, 84.

(45) Otwinoski, Z.; Minor, W. Processing of X-ray Diffraction Data Collected in Oscillation Mode. In *Methods in Enzymology, Vol. 276: Macromolecular Crystallography, Part A*; Carter, C. W., Jr., Sweet, R. M., Eds.; Academic Press: New York, 1997; pp 307−326.

(46) (a) Blessing, R. H. *Acta Crystallogr., Sect. A* **1995**, *51*, 33. (b) Blessing, R. H. *J. Appl. Crystallogr.* **1997**, *30*, 421.

(47) Mackay, S.; Gilmore, C. J.; Edwards, C.; Tremayne, M.; Stuart, N.; Shankland, K. *MaXus: A Computer Program for the Solution and Refinement of Crystal Structures from Diffraction Data*; University of Glasgow: Scotland, Nonius BV: Delft, The Netherlands; and MacScience Co. Ltd.: Yokohama, Japan, 1998.

(48) Sheldrick, G. M. *SHELXTL-97: A Structure Solution and Refinement Program*; University of Göttingen: Germany, 1998.

SHELXTL-97. After all non-hydrogen atoms were located and refined anisotropically, hydrogen atoms on solvent ligands were calculated assuming standard geometries.

In **1**, **2**, and **3**, the basal tetrahedral cobalt atoms are disordered. Disorder in all three compounds was treated in a similar manner (see Supporting Information). One ethyl group (C(61), C(62)) of an Et_2O solvent ligand in **1**, a carbonyl oxygen (O(13)) in **1**, the THF carbon atoms (C(51)−C(54)) in **3**, and three carbons (C(61), C(62), C(64)) of an Et_2O solvent ligand in **3** are disordered. These atoms were split, and their occupancies were refined isotropically. Positions of hydrogen atoms on the disordered solvent ligands were not calculated.

Preparation of $\{(Et_2O)_3Yb[Co_4(CO)_{11}]\}_\infty$, 1. A 50 mL flask was charged with 131 mg (0.241 mmol) of $Hg[Co(CO)_4]_2$ and 25 mg (0.14 mmol) of Yb. Approximately 20 mL of Et_2O was condensed into the flask at −78 °C. The mixture was warmed to room temperature and stirred for several days, during which time the solution became yellow-brown in color and Hg appeared. Infrared spectroscopy was used to monitor the reaction. The reaction solution was frozen at −196 °C, and the presence of noncondensable CO gas was observed manometrically. Filtration of the reaction mixture through Celite gave a red-brown colored filtrate. Dark red-brown flakelike crystals appeared in 14 d after slow evaporation of the solvent at room temperature until 3 mL of solution remained. The mother liquor was removed, and the crystals were washed with 5 mL of Et_2O and 10 mL of hexane. The crystals were dried on the vacuum line for 30 min, yielding 72 mg (63% yield based on $Hg[Co(CO)_4]_2$) of **1**. ^{1}H NMR (250 MHz, d_{10}-Et_2O): δ 3.39 (q, $^3J_{HH}$ = 6.3 Hz, partially hidden by the d_{10}-Et_2O resonance), 1.12 (t, $^3J_{HH}$ = 7.5 Hz, partially hidden by the d_{10}-Et_2O resonance). [59]Co NMR (71.21 MHz, d_{10}-Et_2O): 20 °C, δ −2910 ($\Delta\nu_{1/2}$ = 700 Hz; Co_b); −105 °C, δ −170 ($\Delta\nu_{1/2}$ = 400 Hz; Co_a), −2980 ($\Delta\nu_{1/2}$ = 400 Hz; Co_b). Anal. Calcd for $YbCo_4O_{2.2}C_{4.3}H_7$ (−2.3Et_2O, −9.5CO; sample pumped on for 12 h): C, 10.27; H, 1.40. Found: C, 10.43; H, 1.49.

Preparation of [13C]$\{(Et_2O)_3Yb[Co_4(CO)_{11}]\}_\infty$, [13C]1. Complex **1** (100 mg) was nonselectively labeled by stirring at room temperature a 20 mL Et_2O solution under <1 atm of 99% enriched [13]CO for 7 d. The solution was cooled to −78 °C, and the volatiles were removed under dynamic vacuum. The solution was stirred for another 10 d under <1 atm of [13]CO.[49] ^{13}C NMR (125.8 MHz, d_{10}-Et_2O): 27 °C, δ 214.7 (br s, $CO_{b,t}$), 204.2 (s, $CO_{a,t}$); −110 °C, δ 294.4 (s, η^2,μ_3-CO), 274.8 (s, μ_2-CO), 220.1 (br m, $CO_{b,t}$), 209.2 (br m, $CO_{b,t}$), 207.5 (s, $CO_{b,t}$), 203.8 (s, $CO_{a,t}$).

Preparation of $\{(Et_2O)_3Eu[Co_4(CO)_{11}]\}_\infty$, 2. A 50 mL flask was charged with 203 mg (0.374 mmol) of $Hg[Co(CO)_4]_2$ and 30 mg (0.20 mmol) of Eu, and 30 mL of Et_2O. The mixture was stirred for several days, and the solution turned red-brown in color with Hg and a brown colored oil present. Infrared spectroscopy was used to monitor the reaction. The solution was decanted from the Hg/oil mixture, which was extracted with 2 × 20 mL of Et_2O. The extracts were collected and filtered through Celite. Slow evaporation of the solvent at room temperature (until 3 mL of solution remained) produced after 14 d dark brown rectangular blocklike crystals in a dark brown colored oil. The mother liquor was removed, and the crystals were washed with 2 × 5 mL of Et_2O and 10 mL of hexane. The crystals were vacuum-dried for 30 min, affording 78 mg (45% yield based on $Hg[Co(CO)_4]_2$) of **2**. Anal. Calcd for $EuCo_4O_3C_{4.5}H_5$ (−2.5Et_2O, −8.5CO; sample pumped on for 12 h): C, 10.93; H, 1.02. Found: C, 11.14; H, 1.05.

Preparation of $\{(Et_2O)_2(THF)Yb[Co_4(CO)_{11}]\}_\infty$, 3. The salt [Yb-(THF)$_6$][Co(CO)$_4$]$_2$ (prepared from 0.361 mg, 0.665 mmol of Hg[Co-

$(CO)_4]_2$ and 0.116 mg, 0.670 mmol of Yb metal) was dissolved in 20 mL of Et_2O, and the mixture was stirred for several days. A red-brown colored solution was produced along with a brown colored oil. Infrared spectroscopy was used to monitor the reaction. The volatiles were removed, 20 mL of Et_2O was added, and the mixture was stirred again for 24 h. This procedure was repeated once more. The solution was decanted from the dark brown-black precipitate. Dark red-brown triangular platelike crystals in a brown oil appeared in 7 d after slow evaporation of the solvent at room temperature until 3 mL of solution remained. The mother liquor was removed, and the crystals were washed with 5 mL of Et_2O and 10 mL of hexane. The crystals were dried on the vacuum line for 30 min to afford 221 mg (71% yield based on $Hg[Co(CO)_4]_2$) of **3**. ^{1}H NMR (400 MHz, d_{10}-Et_2O): δ 3.73 (br s, α-H of THF), 3.38 (q, $^3J_{HH}$ = 7.0 Hz, α-H of Et_2O, partially hidden by the d_{10}-Et_2O resonance), 1.83 (br s, β-H of THF), 1.12 (t, $^3J_{HH}$ = 7.2 Hz, β-H of Et_2O, partially hidden by the d_{10}-Et_2O resonance). [59]Co NMR (71.21 MHz, d_{10}-Et_2O): 20 °C, δ −2920 ($\Delta\nu_{1/2}$ = 400 Hz; Co_b). Anal. Calcd for $YbCo_4O_{14}C_{23}H_{28}$ (no loss of solvent or CO; sample pumped on for 30 min): C, 29.48; H, 3.01. Found: C, 29.14; H, 2.97.

Preparation of $\{(THF)_5Eu[Co_4(CO)_{11}]\}_\infty$, 4. The salt [Eu(THF)$_x$]-[Co(CO)$_4$]$_2$ (prepared from 0.212 mg, 0.391 mmol of $Hg[Co(CO)_4]_2$ and 0.061 mg, 0.40 mmol of Eu metal; vide infra) was stirred in 30 mL of Et_2O for several days. A slightly red colored solution was produced, but much of the starting material remained undissolved. Infrared spectroscopy was used to monitor the reaction. The solution was decanted and filtered through Celite. Slow evaporation of the solvent at room temperature (until 2 mL of solution remained) produced dark brown crystals in a red-brown colored oil after 14 d. The oil was removed, and the crystals were washed with 5 mL of Et_2O and 10 mL of hexane. The crystals were dried on the vacuum line for 30 min to afford 42 mg (20% yield based on $Hg[Co(CO)_4]_2$) of **4**. Because of the low yield of **4**, no elemental analysis was performed.

Preparation of [Eu(THF)$_x$][Co(CO)$_4$]$_2$. A 50 mL flask was charged with 217 mg (0.400 mmol) of $Hg[Co(CO)_4]_2$, 61 mg (0.40 mmol) of Eu, and 25 mL of THF. The mixture was stirred for 1 d, during which time the solution became yellow in color and Hg appeared. The solution was filtered through Celite to give a yellow colored filtrate. The THF was removed in vacuo, and the resulting oil was washed with 2 × 10 mL of hexane. After the mixture was vacuum-dried for 30 min, 201 mg of a tan solid was obtained. Although X-ray-quality crystals of [Eu(THF)$_x$][Co(CO)$_4$]$_2$ could not be grown, the solid-state (KBr) IR spectra of [Yb(THF)$_6$][Co(CO)$_4$]$_2$ and [Eu(THF)$_x$][Co(CO)$_4$]$_2$ are nearly identical. Anal. Calcd for $EuCo_2O_8C_{16.25}H_{22}$ ([Eu(THF)$_{2.75}$][Co-(CO)$_{2.625}$]$_2$; sample pumped on for 3 h): C, 31.73; H, 3.60. Found: C, 31.97; H, 3.70.

Supporting Information Available: Molecular structures (ORTEPs), discussions of disorder, relevant solution and solid-state IR spectra (PDF). Four X-ray crystallographic files in CIF format. This material is available free of charge via the Internet at http://pubs.acs.org.

JA0304852

(49) Darensbourg, D. J. In *The Chemistry of Metal Cluster Complexes*; Shriver, D. F., Kaesz, H. D., Adams, R. D., Eds.; VCH: New York, 1990; pp 185−189.

(50) Albano, V. G.; Ciani, G.; Fumagalli, A.; Martinengo, S.; Anker, W. M. *J. Organomet. Chem.* **1976**, *116(3)*, 343−52.